How to cite: *Angew. Chem. Int. Ed.* **2020**, *59*, 17388–17392
International Edition: doi.org/10.1002/anie.202007653
German Edition: doi.org/10.1002/ange.202007653

Ring Systems | Hot Paper

An Adduct of Sulfur Monoxide to a Frustrated Sn/P Lewis Pair

*Philipp Holtkamp, Timo Glodde, Dario Poier, Beate Neumann, Hans-Georg Stammler, and Norbert W. Mitzel**

Dedicated to Professor F. Ekkehardt Hahn on the occasion of his 65th birthday

Abstract: *The geminal frustrated Lewis pair $(F_5C_2)_3SnCH_2P(tBu)_2$ (**1**) reacted with N-sulfinylaniline PhNSO to afford the first sulfur monoxide adduct of a main group metal, $(F_5C_2)_3SnCH_2P(tBu)_2{\cdot}SO$ (**2**), which contains a SnCPSO ring. The second product is a phenylnitrene adduct of **1**. The surprising stability of **2** was compared with the stabilities of the so far inaccessible O_2 and S_2 adducts of **1**. Attempts to prepare these from **1** and the elemental chalcogens (O_2, S_8, Se_∞, Te_∞) led to four-membered SnCPE ring systems. Quantum-chemical investigations of **2** demonstrate the bond polarity of the SO unit to stabilize **2**.*

The chemistry of sulfur(II)oxide, SO, is currently experiencing a renaissance. SO itself is highly unstable in higher concentrations and in the condensed phase, but observed as component of the dilute atmospheres of celestial bodies in outer space. It is perfectly stable as an isolated molecule, provided it does not interfere with reactive partners. The spectroscopic properties of SO and some of its excited states have been studied in detail by high-resolution spectroscopy.[1]

For a long period of time, the chemistry of SO was explored mainly as a complex ligand in transition metal chemistry.[2] The SO ligand was often generated from thionyl chloride by reduction in the coordination sphere of the metal atom. Complexes with terminal S-bound sulfur monoxide are known[3] as well as with a bridging ligand between two metal atoms (e.g. $[Cp(CO)_2Mn]_2SO$[4]).

Only recently, methods were developed to transfer SO from nitrogen-bound forms, in particular sulfinylimine-type compounds.[5] Cummins et al. found a way of SO transfer from an anthracene-based *N*-sulfinylhydrazine onto 3,5-di-*tert*-butyl-1,2-benzoquinone and 2,3-dimethyl-1,3-butadiene at elevated temperature.[6] This was preceded by work of Stephan et al., who observed adduct formation between the readily available *N*-sulfinyl-*p*-toluidine, *p*-TolNSO, and the frustrated Lewis pairs (FLPs) $P(tBu)_3/B(C_6F_5)_3$ and $[(Mes)_2P(CH_2)_2B(C_6F_5)_2]$; the adducts contain P-N(*p*-Tol)-S-O-B units. They demonstrated the adduct $[(Mes)_2P(CH_2)_2B(C_6F_5)_2]{\cdot}$*p*-TolNSO to be able to transfer an SO unit to the rhodium complex $[RhCl(PPh_3)_3]$ and to a *N*-heterocyclic carbene.[7]

The binding of complete *N*-sulfinylamine units to a FLP was earlier demonstrated by Erker et al., who generated an adduct with an intramolecular Zr^+/P FLP system, whereby the still intact PhNSO unit binds to P with N and to Zr side-on with an S-O unit.[8]

Despite these activities in SO chemistry, the trapping of a complete S-O unit by a main group metal system has not been achieved so far, but occurred when we reacted our recently reported Sn/P FLP $(F_5C_2)_3SnCH_2P(tBu)_2$ (**1**) with *N*-sulfinylaniline PhNSO.[9] FLP **1** is the heaviest congener of a series of tetrel-based FLP systems $(F_5C_2)_3ECH_2P(tBu)_2$ (E = Si, Ge, Sn (**1**)), with large differences in their reactivity.[9,10] Due to its relatively soft Lewis acid binding site, the Sn/P FLP **1** is, for instance, capable of reversibly binding CO_2.[9] Its affinity towards oxygen atoms is obviously less pronounced than in systems with much harder acid sites like those based on boron, aluminum, or silicon. It was thus of interest whether a soft-acid FLP binds or cleaves a substrate differently than a hard-acid FLP.

The reaction of **1** with *N*-sulfinylaniline does not result in addition of the whole PhNSO unit, but in the formation of an SO adduct to FLP **1** (Scheme 1). Adduct **2** represents, to the best of our knowledge, the first example of an SO complex to an FLP and to a main group metal, here tin. ^1H and ^{13}C NMR spectroscopic investigations of product **2** proved the absence of signals of a phenyl group and the ^1H NMR spectrum shows a characteristic doublet ($^2J_{P,H} = 6$ Hz) for the CH_2 protons of

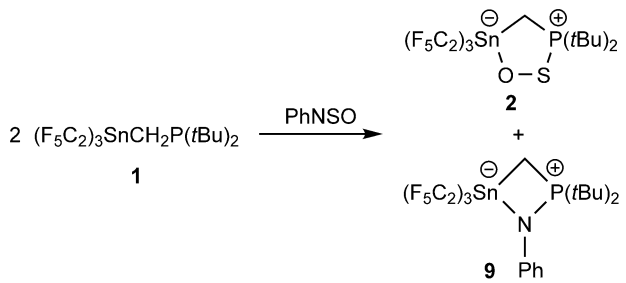

Scheme 1. Reaction of FLP **1** with PhNSO.

[*] M. Sc. P. Holtkamp, M. Sc. T. Glodde, M. Sc. D. Poier, B. Neumann, Dr. H.-G. Stammler, Prof. Dr. N. W. Mitzel
Lehrstuhl für Anorganische Chemie und Strukturchemie
Fakultät für Chemie, Universität Bielefeld
Universitätsstraße 25, 33615 Bielefeld (Germany)
E-mail: mitzel@uni-bielefeld.de
Supporting information and the ORCID identification number(s) for the author(s) of this article can be found under: https://doi.org/10.1002/anie.202007653.

an adduct at 1.11 ppm. The molecular structure of adduct **2** obtained by X-ray diffraction analysis (Figure 1) exhibits a five-membered SnCPSO heterocycle and the formation of an unusual SO adduct under loss of the N-Ph unit.

Adduct **2** crystallizes with four slightly different molecules in the asymmetric unit. They define a range of structural parameters that are possible for this molecule (for more details see the Supporting Information). The considerably strong distortion of the different coordination spheres of the tin atoms is described by τ_{Sn} parameters in the range between 0.38 and 0.78 (Table 1). These are calculated by subtracting the two largest bond angles at Sn and dividing the result by 60°. τ_{Sn} parameters close to 1 indicate a trigonal-bipyramidal coordination sphere, while those close to 0 indicate a square-pyramidal one.[11]

The S–O bond lengths in **2** between 1.604(5) and 1.615(4) Å are unusually long: more than 0.1 Å longer than in gaseous SO ($r_e = 1.481(1)$ Å, determined by high-resolution IR spectroscopy),[12] gaseous SO_2 ($r_e = 1.430793(4)$ Å determined by gas electron diffraction), and also longer than the endocyclic S–O bond in the corresponding adduct **1**·SO_2 (1.524(1) Å).[9] The latter correlates with significantly shorter Sn–O (2.122(4)–2.131(4) Å) and P–S (2.082(2)–2.089(2) Å) bonds in **2** compared to **1**·SO_2 at 2.239(1) and 2.331(1) Å, respectively.[9]

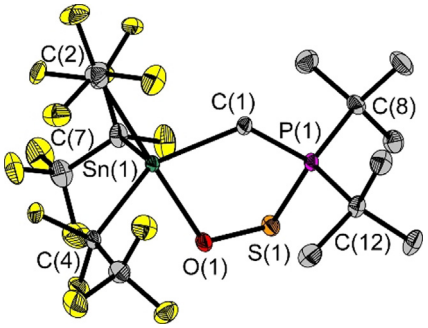

Figure 1. Molecular structure of one conformer of compound **2** in the solid state. Ellipsoids are set at 50% probability; hydrogen atoms are omitted for clarity. Selected bond lengths [Å] and angles [°]: S(1)-P(1) 2.084(2), S(1)-O(1) 1.615(4), P(1)-C(1) 1.787(5), P(1)-C(8) 1.855(5), P(1)-C(12) 1.853(5), Sn(1)-C(1) 2.183(5), Sn(1)-C(2) 2.297(5), Sn(1)-C(4) 2.227(5), Sn(1)-C(7) 2.231(5); P(1)-C(1)-Sn(1) 113.9(2), C(1)-P(1)-S(1) 104.2(2), O(1)-S(1)-P(1) 101.2(1), S(1)-O(1)-Sn(1) 116.4(2), O(1)-Sn(1)-C(2) 176.2(2), O(1)-Sn(1)-C(4) 83.5(2), O(1)-Sn(1)-C(7) 91.6(2), O(1)-Sn(1)-C(1) 86.6(2).

Table 1: Selected NMR and structural parameters of compounds **2**–**9**.

	$\delta(^{31}P)$ [ppm][a]	$\delta(^{119}Sn)$ [ppm][a]	$^2J_{Sn,P}$ [Hz][a]	∡(Sn-C-P) [°]	τ_{Sn}[b]
2	78.0	−265.2	68	113.9(2)–114.9(2)	0.38–0.78
3	78.4	−315.5	–	93.9(1)	0.46
4	79.0	−335.0	141	103.0(2)	0.50/0.17
7	73.0	−380.4	128	–	–
8	43.6	−482.1	83	–	–
9	56.3	−330.7	117	97.6	0.55

[a] In C_6D_6 at ambient temperature. [b] Calculated according to Addison et al.[11]

In this respect, the S–O bond in **2** compares better with the long S–O bonds in the rarely described sulfenic acid esters (RSOR′); an example is *o*-nitrobenzenesulfenate with an S–O bond length of 1.65 Å.[13] Sulfenic acid esters are much less stable than their sulfoxide isomers (RR′S = O); the existence of **2** in this Sn-O-S-P bonded form rather than the sulfoxide form SnS(=O)P is thus neither self-evident nor easy to predict. It becomes apparent that SO experiences a much stronger change in bonding than SO_2, when it is incorporated into an adduct to FLP **1**.

In line with the partial charge distribution $^{\delta+}S{=}O^{\delta-}$ in sulfur monoxide, its negative end binds to the Lewis acid and its positive to the Lewis base. One could have speculated that a reversed orientation would be favored, because the relatively soft binding site (according to HSAB)[14] of the acid function, the tin atom, could prefer to bind to sulfur instead of oxygen.

SO adduct **2** is a stable and storable substance. Expected signs of instability would be, for instance, the extrusion of S_8 with formation of an oxygen adduct **1**·O (**3**). The question arose whether related adducts of homodichalcogens **1**·O_2 (**5**) and **1**·S_2 (**6**) would be feasible synthetic targets and whether they would be as stable as the adduct of the heterodichalcogen SO. While reactions of FLP systems with the heavier chalcogens S, Se, and Te have been comparatively well studied,[15] those with gaseous O_2 are limited to a few examples.[16]

Uhl et al. used a geminal Al/P FLP system and observed the formation of four-membered AlCPE (E = S, Se, Te) heterocycles; the corresponding Se and Te derivatives form dimers in the solid state due to closed-shell chalcogen–chalcogen interactions.[15a,b] Driess et al. attempted to realize an O_2 adduct with SiOOB subunit by reacting a xanthendiyl-based B/Si^{II} FLP with dioxygen,[16a] but instead obtained a monooxygenated species bearing a Si=O···B-type interaction, as was also observed for the reactions with CO_2, N_2O, and H_2O.[16a] Bourissou et al. reacted an *o*-phenylene-bridged B/P FLP with singlet O_2, after observing no reaction with triplet O_2, and found an adduct of P-O-B-OR-type (R = Mes, Pin) and speculated about an intermediate O-O-bridge-type adduct.[16b]

The exposure of a *n*-hexane solution of **1** to O_2 results in the immediate precipitation of a colorless solid, the monooxygen adduct **1**·O (**3**) (Scheme 2). Single-crystal X-ray diffraction (Figure 2) reveals **3** to contain a four-membered SnCPO heterocycle. It has a significantly narrower Sn(1)-C(7)-P(1) angle of 93.9(1)°, compared to adduct **2**. Compared to the monooxygenated homologous Si and Ge derivatives, obtained by reacting the corresponding Si and Ge FLPs with NO, the structure of **3** resembles the closed ring structure of

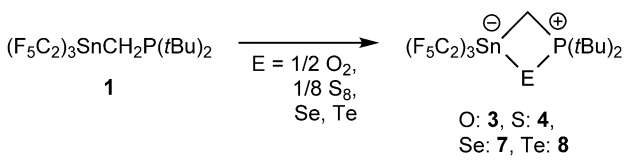

Scheme 2. Reaction of FLP **1** with elemental chalcogens.

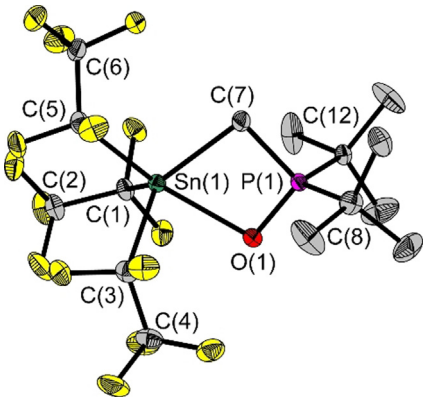

Figure 2. Molecular structure of compound **3** in the solid state. Ellipsoids are set at 50% probability; hydrogen atoms are omitted for clarity. Selected bond lengths [Å] and angles [°]: P(1)-C(7) 1.807(2), P(1)-C(8) 1.842(2), P(1)-O(1) 1.532(2), Sn(1)-O(1) 2.329(2), Sn(1)-C(1) 2.218(2), Sn(1)-C(5) 2.275(2), Sn(1)-C(7) 2.184(2); P(1)-C(7)-Sn(1) 93.9(1), C(7)-P(1)-C(8) 108.4(1), P(1)-O(1)-Sn(1) 96.4(1), O(1)-Sn(1)-C(1) 90.1(1), O(1)-Sn(1)-C(5) 164.0(1), O(1)-Sn(1)-C(7) 69.3(1).

the Si/P FLP monooxygen adduct rather than the open-chain structure of the Ge/P FLP monooxygen adduct.[10b] The P–O and Sn–O bond lengths of **3** are 1.532(1) and 2.329(1) Å, respectively. A τ_{Sn} parameter of 0.46 indicates a clearly distorted square-pyramidal coordination at the tin atom.

Similar to the oxygen product **3** and results of Uhl et al.,[15a,b] the reaction of **1** with the heavier chalcogens led to the formation of the respective four-membered SnCPE (E = S, Se, Te) heterocycles (Scheme 2). The molecular structure of the monosulfur adduct **1**·S (**4**) was determined by X-ray diffraction (Figure 3) with all C_2F_5 groups disordered at two positions with a ratio of 64:36, while a stronger disorder of the adducts **1**·Se (**7**) and **1**·Te (**8**), prevented their reasonable structural elucidation. Compared to the adduct **1**·O (**3**), the Sn(1)-C(7)-P(1) angle in **4** at 103.0(2)° is clearly wider and the Sn(1)-E(1)-P(1) angle (E = S: 80.7(1)°; E = O: 96.4(1)°) is significantly narrower. This correlates with inherently longer P(1)-S(1) and Sn(1)-S(1) bonds of 2.010(2) and 2.735(2) Å, respectively.

The corresponding chalcogen adduct formation can also be verified in all NMR spectra according to certain trends (Table 1). Most affected are the protons and carbon atom of the CH_2 unit as well as the tin and phosphorus nuclei. While the ^{1}H NMR signal of the methylene protons is shifted to lower field for heavier chalcogens, a high-field shift of the ^{31}P and ^{119}Sn NMR resonances is observed along the same series (Table 1).

To answer the question why the formation of an S-O bridge is preferred and the product stable, while the reactions of **1** with O_2 give no corresponding O-O bridge or reactions with S_8, no S-S bridge (or a longer S_n bridge), we performed quantum-chemical calculations at the PBE0-D3/def2TZVPP level of theory (for details see the Supporting Information). Scheme 3 shows several calculated molar free reaction enthalpies for adduct formations and interconversion of the adducts. They show that the formations of all isolated adducts **2**–**4** and the conceivable adducts **1**·O_2 (**5**) and **1**·S_2 (**6**) are exergonic processes. Formation of **3** is the most exergonic ($\Delta G = -289$ kJ mol^{-1}), followed by the incorporation of ^{3}SO and $^3O_2$ with −145 and −122 kJ mol^{-1}, respectively. Adduct formations with elemental sulfur leading to **1**·S (**4**) and **1**·S_2 (**6**) are the energetically least favored processes with −109 and −59 kJ mol^{-1}, respectievely. It is not excluded that the species **1**·O_2 (**5**) and **1**·S_2 (**6**) represent intermediates in the formation of the isolated adducts **3** and **4**. However, the case of the SO adduct **2** is surprising: it is thermodynamically stable towards extrusion of O_2, but not towards loss of sulfur.

The effect of polarity in the S–O bond in **2** relative to the nonpolar bonds in **5** and **6** becomes apparent when one calculates the situation-specific covalent radii from the homonuclear bonds and uses them to predict the S–O bond length at 1.747 Å. This is 0.16 Å longer than the DFT-predicted S–O bond length for **2** (1.588 Å, compare XRD: 1.604(5)–1.615(4) Å), indicating a highly stabilizing effect due to bond polarity. NPA charge calculations suggest that both oxygen and sulfur atoms in the homodichalcogen adducts **5**

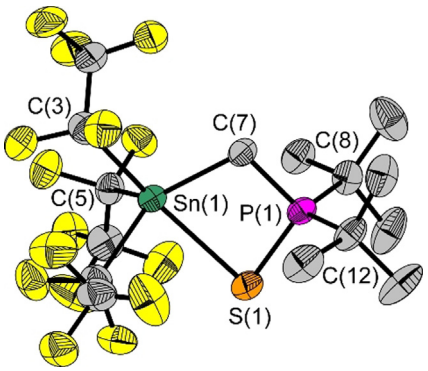

Figure 3. Molecular structure of compound **4** in the solid state. Ellipsoids are set at 30% probability; hydrogen atoms and minor occupied disordered C_2F_5 groups are omitted for clarity. Selected bond lengths [Å] and angles [°]: P(1)-C(7) 1.801(5), P(1)-C(8) 1.844(6), P(1)-S(1) 2.010(2), Sn(1)-S(1) 2.735(2), Sn(1)-C(1) 2.244(11), Sn(1)-C(3) 2.275(12), Sn(1)-C(7) 2.176(6); P(1)-C(7)-Sn(1) 103.0(2), C(7)-P(1)-C(8) 108.0(3), P(1)-S(1)-Sn(1) 80.7(1), S(1)-Sn(1)-C(1) 87.0(3), S(1)-Sn(1)-C(3) 163.8(3), S(1)-Sn(1)-C(7) 73.6(1).

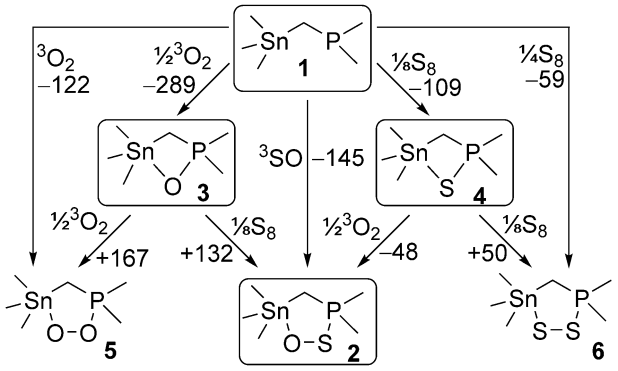

Scheme 3. Quantum-chemically calculated reactions of FLP **1** with dichalcogens and some interconversions along with their free enthalpies (in kJ mol^{-1}). The substituents at Sn and P are omitted for simplicity. The compounds in boxes were so far experimentally observed.

and **6** carry negative charges, whereas in the SO adduct **2** the oxygen atom is negatively and the sulfur atom positively charged. The bond critical point (BCP) between the tin and oxygen atoms in adduct **2** is characterized by a low charge density and a negative Laplacian, indicating a donor–acceptor interaction between the electrophilic tin and the nucleophilic oxygen atom (Figure 4). In contrast, characteristics of a covalent and polarized bond are found for the P–S and S–O bonds, respectively (more details see the Supporting Information).

In the adducts **5** and **6**, however, the homoatomic dichalcogen bonds O–O and S–S are characterized as shared and covalent bonds, respectively. This is exemplified by kinetic energy density ratios of 0.77 and 0.39 for **5** and **6**, respectively. For all cases, the QTAIM analysis suggests a nonovalent donor–acceptor interaction for interactions between Sn and O/S. Therefore, according to NPA charge calculations and QTAIM analysis, the stability of adduct **2** can qualitatively be explained by the polarity and strength of the S–O bond, which is induced by the electron-withdrawing character of the Lewis acidic tin atom.

The second product of the reaction of **1** with PhNSO could be identified in the better soluble part of the reaction mixture (Scheme 1). Besides traces of PhNSO and adduct **2**, a second adduct-type species **9** was found. Its ^{31}P NMR resonance at 56.3 ppm is slightly high-field shifted compared to SO adduct **2** ($\delta(^{31}P) = 78.0$ ppm, Table 1). Signals of a phenyl group in the ^{1}H NMR spectrum between 6.80 and 7.19 ppm suggest that **9** contains the Ph-N part of PhNSO. Structure determination by single-crystal X-ray diffraction showed **9** to be a 1,1-adduct of phenylnitrene, Ph-N, to **1**. Its molecular structure (Figure 5) reveals a four-membered SnCPN heterocycle with a Sn(1)-C(7)-P(1) angle of 97.6(2)°, similar to those of the four-membered heterocycles in **3** and **4**. The opposing Sn(1)-N(1)-P(1) angle has a similar value, 96.7(1)°, and the sum of angles at N(1) of 359.9(5)° proves its planar coordination. The τ_{Sn} parameter of 0.55 implies a strongly distorted trigonal-bipyramidal coordinate tin atom (Table 1).

In essence we have found a way to transfer the intact sulfur monoxide (SO) unit of *N*-sulfinylaniline to a tin/phosphorus FLP, leaving a nitrene-FLP adduct as a second product. This first main group metal adduct of SO is surprisingly stable, whereas other dichalcogen adducts like **1**·O_2 (**5**) and **1**·S_2 (**6**) are yet inaccessible and reactions of

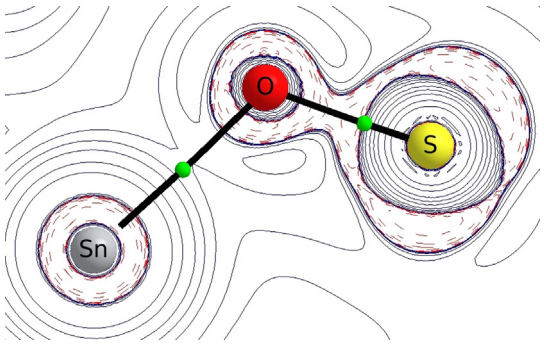

Figure 4. Calculated Laplacian plot of **2**. The BCPs are displayed in green. The curvatures indicate a donor–acceptor interaction between O and Sn. The BCP between O and S indicates a polar bond.

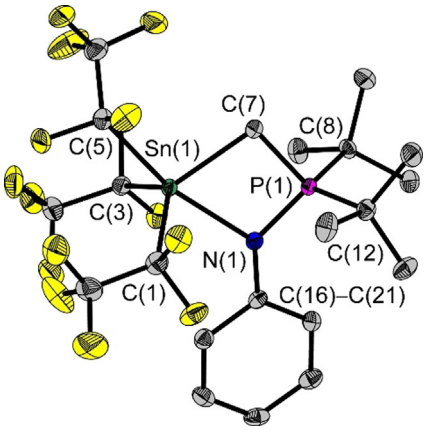

Figure 5. Molecular structure of compound **9** in the solid state. Ellipsoids are set at 50% probability; hydrogen atoms are omitted for clarity. Selected bond lengths [Å] and angles [°]: P(1)-C(7) 1.798(3), P(1)-C(8) 1.881(3), P(1)-N(1) 1.644(3), Sn(1)-N(1) 2.312(3), Sn(1)-C(1) 2.263(4), Sn(1)-C(5) 2.297(4), Sn(1)-C(7) 2.163(3), C(16)-N(1) 1.407-(4); P(1)-C(7)-Sn(1) 97.6(2), C(7)-P(1)-N(1) 95.9(2), P(1)-N(1)-C(16) 131.7(2), P(1)-N(1)-Sn(1) 96.7(1), Sn(1)-N(1)-C(16) 131.5(2), N(1)-Sn(1)-C(1) 91.9(1), N(1)-Sn(1)-C(5) 166.8(1), N(1)-Sn(1)-C(7) 69.6(1).

1 with the elemental chalcogens lead to the monochalcogen adducts. The relative stability of **2** is primarily attributed to the SO units' polarity, as quantum-chemical calculations show. These results encourage us in future work to further investigate the capability of FLP **1** to capture and transfer reactive or transient species.

Acknowledgements

We thank Erik Stratmann for lab assistance, Marco Wissbrock for recording NMR spectra and Barbara Teichner for performing elemental analyses. We gratefully acknowledge financial support from Deutsche Forschungsgemeinschaft (DFG, grant MI477/31-1 project no. 320753677 and core facility GED@BI grant MI477/35-1 project no. 324757882) and computing time provided by the Paderborn Center for Parallel Computing (PC^2). Open access funding enabled and organized by Projekt DEAL.

Conflict of interest

The authors declare no conflict of interest.

Keywords: fluoroalkyl groups · frustrated Lewis pairs · sulfur monoxide · tin

[1] a) N. N. Greenwood, A. Earnshaw, *Chemistry of the Elements*, 2nd ed., Butterworth-Heinemann, Amsterdam, **1997**; b) E. Wiberg, *Lehrbuch der Anorganischen Chemie*, Walter de Gruyter & Co., Berlin, **1964**; c) C. A. Gottlieb, E. W. Gottlieb, M. M. Litvak, J. A. Ball, H. Pennflied, *Astrophys. J.* **1978**, *219*, 77–94; d) F. Salama, H. Frei, *J. Phys. Chem.* **1989**, *93*, 1285–1292.

[2] W. A. Schenk, *Angew. Chem. Int. Ed. Engl.* **1987**, *26*, 98 – 109; *Angew. Chem.* **1987**, *99*, 101 – 112.
[3] a) W. A. Schenk, J. Leissner, C. Burschka, *Angew. Chem. Int. Ed. Engl.* **1984**, *23*, 806 – 807; *Angew. Chem.* **1984**, *96*, 787 – 788; b) W. A. Schenk, J. Leissner, C. Burschka, *Z. Naturforsch. B* **1985**, *40*, 1264 – 1273; c) I.-P. Lorenz, W. Hiller, M. Conrad, *Z. Naturforsch. B* **1985**, *40*, 1383 – 1389.
[4] I.-P. Lorenz, J. Messelhäuser, W. Hiller, M. Conrad, *J. Organomet. Chem.* **1986**, *316*, 121 – 138.
[5] a) G. Kresze, W. Wucherpfennig, *Angew. Chem. Int. Ed. Engl.* **1967**, *6*, 149 – 167; *Angew. Chem.* **1967**, *79*, 109 – 127; b) R. M. Romano, C. O. Della Védova, R. Boese, *J. Mol. Struct.* **1999**, *475*, 1 – 4; c) R. M. Romano, C. O. Della Védova, *J. Mol. Struct.* **2000**, *522*, 1 – 26.
[6] M. Joost, M. Nava, W. J. Transue, M.-A. Martin-Drumel, M. C. McCarthy, D. Patterson, C. C. Cummins, *Proc. Natl. Acad. Sci. USA* **2018**, *115*, 5866 – 5871.
[7] L. E. Longobardi, V. Wolter, D. W. Stephan, *Angew. Chem. Int. Ed.* **2015**, *54*, 809 – 812; *Angew. Chem.* **2015**, *127*, 823 – 826.
[8] X. Xu, G. Kehr, C. G. Daniliuc, G. Erker, *J. Am. Chem. Soc.* **2014**, *136*, 12431 – 12443.
[9] P. Holtkamp, F. Friedrich, E. Stratmann, A. Mix, B. Neumann, H.-G. Stammler, N. W. Mitzel, *Angew. Chem. Int. Ed.* **2019**, *58*, 5114 – 5118; *Angew. Chem.* **2019**, *131*, 5168 – 5172.
[10] a) B. Waerder, M. Pieper, L. A. Körte, T. A. Kinder, A. Mix, B. Neumann, H.-G. Stammler, N. W. Mitzel, *Angew. Chem. Int. Ed.* **2015**, *54*, 13416 – 13419; *Angew. Chem.* **2015**, *127*, 13614 – 13617; b) T. A. Kinder, R. Pior, S. Blomeyer, B. Neumann, H.-G. Stammler, N. W. Mitzel, *Chem. Eur. J.* **2019**, *25*, 5899 – 5903.
[11] A. W. Addison, T. N. Rao, J. Reedjik, J. van Rijn, G. C. Verschoor, *J. Chem. Soc. Dalton Trans.* **1984**, 1349 – 1356.
[12] E. Tiemann, *J. Mol. Spectrosc.* **1982**, *91*, 60 – 71.
[13] W. C. Hamilton, S. J. Laplaca, *J. Am. Chem. Soc.* **1964**, *86*, 2289 – 2290.
[14] R. G. Pearson, *J. Am. Chem. Soc.* **1963**, *85*, 3533 – 3539.
[15] a) W. Uhl, J. Possart, A. Hepp, M. Layh, *Z. Anorg. Allg. Chem.* **2017**, *643*, 1016 – 1029; b) W. Uhl, P. Wegener, M. Layh, A. Hepp, E.-U. Würthwein, *Organometallics* **2015**, *34*, 2455 – 2462; c) D. Holschumacher, C. G. Daniliuc, P. G. Jones, M. Tamm, *Z. Naturforsch. B* **2011**, *66*, 371 – 377.
[16] a) Z. Mo, T. Szilvási, Y.-P. Zhou, S. Yao, M. Driess, *Angew. Chem. Int. Ed.* **2017**, *56*, 3699 – 3702; *Angew. Chem.* **2017**, *129*, 3753 – 3756; b) S. Porcel, G. Bouhadir, N. Saffon, L. Maron, D. Bourissou, *Angew. Chem. Int. Ed.* **2010**, *49*, 6186 – 6189; *Angew. Chem.* **2010**, *122*, 6322 – 6325.
[17] 2006136, 2006137, 2006138, 2006139 contain the supplementary crystallographic data for this paper. These data are provided free of charge by the joint Cambridge Crystallographic Data Centre and Fachinformationszentrum Karlsruhe Access Structures service www.ccdc.cam.ac.uk/structures..

Manuscript received: May 28, 2020
Accepted manuscript online: June 18, 2020
Version of record online: August 6, 2020

